NOTAS DE FÍSICA

VOLUME XI

Nº 2

π^-p INTERACTIONS AT 4.0 GeV/c

by

L. Bondár, K. Bongartz, M. Deutschmann, E. Keppel, G. Kraus, H. Weber, D. C. Colley, W. P. Dodd, J. Simmons, B. Tallini; D. Cords, Ch. Dehne, E. Lohrmann, P. Soding, M. Teucher, G. Wolf, J. M. Brownlee, I. Butterworth, F. I. Campayne, M. Ibbotson, N. N. Biswas, I. Derado, K. Gottstein, D. Lüers, G. Lütjens, N. Schmitz, B. Nellen, G. Winter and A. M. Freire-Endler

CENTRO BRASILEIRO DE PESQUISAS FÍSICAS

Av. Wenceslau Braz, 71

RIO DE JANEIRO

1963

Notas de Física - Volume XI- Nº 2

$\pi^- p$ INTERACTIONS AT 4.0 GeV/c

L. Bondár, K. Bongartz, M. Deutschmann, E. Keppel,
G. Kraus, H. Weber
Physikalisches Institut der Technischen Hochschule-Aachen

D. C. Colley, W. P. Dodd, J. Simmons, B. Tallini *
Physics Department, University of Birmingham - Birmingham

D. Cords, Ch. Dehne, E. Lohrmann, P. Soding, M. Teucher,
G. Wolf
Physikalisches Staatinstitut
II. Institut für Experimentalphysik,
Hamburg and DESY - Hamburg

J. M. Brownlee, I. Butterworth, F. I. Campayne, M. Ibbotson
Imperial College of Science and Tecnology - London

N. N. Biswas, I. Derado, K. Gottstein,
D. Lüers, G. Lütjens, N. Schmitz
Max-Planck-Institut für Physik and Astrophysik - Munchen

B. Nellen, G. Winter
Physikalisches Institut der Universität Bonn and KFA Julich-Bonn

A. M. Freire-Endler **
Centro Brasileiro de Pesquisas Físicas, Rio de Janeiro - Brazil

(Received October 18, 1963)

---

* At present on leave of absence at the Centre des Etudes Nucléaires, Saclay.

** This work was done when the author was at Physikalisches Institut der Universität Bonn.

Summary: A bubble chamber investigation of π^- p interactions has been carried out at a momentum of 4 GeV/c. Analysis is limited to 3828 events with two charged secondaries. Cross sections, angular distributions and momentum distributions for the different reactions are presented. Four-momentum transfer distributions for elastic scattering and single pion production are discussed. The production of pion resonant states is investigated.

* * *

1. Introduction

In this paper further results on the π^- meson interaction with protons at an incident momentum of 4 GeV/c are presented. Discussion is limited to events with two prongs, i.e. two charged secondaries. Four prong events have formed the subject of a previous report [1] hereafter referred to as I. The reactions involved are thus:

$$(1)\quad \pi^- p \longrightarrow p\,\pi^-$$

$$(2a)\quad \pi^- p \longrightarrow p\,\pi^-\,\pi^0$$

$$(2b)\quad \pi^- p \longrightarrow n\,\pi^+\,\pi^-$$

$$(3a)\quad \pi^- p \longrightarrow p\,\pi^-\,(m\,\pi^0)\quad m \geqslant 2$$

$$(3b)\quad \pi^- p \longrightarrow n\,\pi^+\,\pi^-\,(m\,\pi^0),\quad m \geqslant 1$$

Analysis of events was carried out by means of kinematic fitting and bubble density measurement in a way identical to that described in I. About 5% of the events failed to pass through the geometry programme in spite of repeated measurements. At momenta in excess of 1.7 GeV/c it was not possible

to identify positive tracks from their bubble density. The only serious consequence of this fact was that about 25% of the events which gave a fit to reactions (2b) were also kinematically consistent with the unfittable reaction (3a). All these events have been classified as due to reaction (2b). The effective mass distributions resulting from these particular events agree with these resulting from the completely unambiguous events.

2. Cross Sections

Table I gives the total number of events and cross-sections for each channel.

Table I

Channel	N° of Events Analysed	Corrected Cross-section in mb
$p\ \pi^-$	1083	6.62 ± 0.22
$p\ \pi^-\pi^o$	446	2.21 ± 0.10
$n\ \pi^+\pi^-$	636	3.16 ± 0.13
$p\ \pi^-(m\ \pi^o)$	538	2.67 ± 0.12
$n\ \pi^+\pi^-(m\ \pi^o)$	1125	5.57 ± 0.17
Total	3828	20.23 ± 0.30

The total two prong cross-section is based on the total number of events found. The usual corrections for beam contamination (about 5% muons, 1% antiprotons), scanning efficiency, etc., have been made.

In the case of the elastic cross-section, a 13% correction has been made for the loss of events at small scattering angles. This correction is discussed in the next section. A hydrogen density of 0.0625 gr/cm^3 has been used. All the errors quoted are statistical.

The high cross-section for the reaction $\pi^- p \longrightarrow n\, \pi^+\pi^-(m\pi^o)$ may indicate that ω^o production together with a neutron has an appreciable cross-section.

3. Elastic Scattering

Fig. 1 shows the differential cross-section $\partial\sigma/\partial t$ for elastic scattering as a function of $-t$, where t is the four-momentum transfer to the proton in GeV^2. To correct for scanning loss the distribution of the angle ϕ between the normal to the scattering plane and the optic axis of the cameras was plotted. Loss of events at values of ϕ approaching 90^o could thus be estimated. At values of $-t < 0.02$ GeV^2 the correction approaches 100% and there is also an additional loss of events due to the shortness of the recoil proton track, hence these events have not been included. For $0.02\ \text{GeV}^2 < -t < 0.04\ \text{GeV}^2$ a correction factor of 1.20 had to be applied, for $0.04\ \text{GeV}^2 < -t < 0.06\ \text{GeV}^2$ a factor of 1.08 and for $-t > 0.06$ GeV^2 correction was small and not statistically significant.

The data are consistent with an exponential distribution of the differential cross-section $\partial\sigma/\partial t = C\, e^{A\,t}$. A least

squares fit over the region 0.02 GeV^2 < - t <0,4 GeV^2 yields a value for C of (52.8 ± 3.96) mb/GeV^2 and a value for A of (8.53 ± 0.49)(GeV)$^{-2}$. The probability from a χ^2 -test was 10%. This fit is shown in Fig. 1b. At an incident pion momentum of 4.13 GeV/c Ting at al[2] obtain a value for A of (8.0 ± 0.5) (GeV)$^{-2}$ in the range 0.07 GeV^2 < - t < 0.4 GeV^2, the present data fitted over the same range of t gives a value of (7.22 ± 0.060) (GeV)$^{-2}$. These two values are consistent, and our value for A is consistent with the general compilation of A values given by Brandt et al[3].

If, following Brandt et al we fit the data to $C'e^{A't + B't^2}$ in the region 0.02 GeV^2 < - t < 0.4 GeV^2 the values of the constants are:

$$C' = (68.8 \pm 7.86) \text{ mb/GeV}^2$$
$$A' = (12.91 \pm 1.61) \text{ (GeV)}^{-2}$$
$$B' = (12.67 \pm 4.33) \text{ (GeV)}^{-4}$$

with a χ^2 - probability of 40%.

There is no evidence for a backwards diffraction peak.

The fitted line in Fig. 1b has been used to derive the corrected total elastic cross-section given above.

The optical theorem point shown in Fig. 1 (O.T.P.), is deduced from the total cross-section of (32.3 ± 0.7 mb) found in the present experiment. The extrapolation of $\partial\sigma/\partial t$ to t = = 0 intersects the axis just below the optical theorem point such that $\left|\frac{\text{Re } f(0)}{\text{Im } f(0)}\right|^2 = -0.011 \pm 0.08$. If the total cross-

section of (30.5 ± 0.5) mb found in counter experiments [4,5,6] is used to derive the optical point one finds $\left|\frac{\text{Re } f(0)}{\text{Im } f(0)}\right|^2 =$ = 0.11 ± 0.09.

4. Four-Momentum Transfer in Single Pion Production

The single pion production channels are largely dominated by pion resonances and at least in these regions one expects the reactions to be mainly described by the single pion exchange process of Fig. 2 [7].

Fig. 3 shows the distribution of the four-momentum transfer to the proton, t, in the cases where the events are consistent with:

$\pi^- p \longrightarrow p + \rho^-$ (700 MeV < $M_{\pi^-\pi^0}$ < 820 MeV)

$\pi^- p \longrightarrow n + \rho^0$ (700 MeV < $M_{\pi^+\pi^-}$ < 820 MeV)

$\pi^- p \longrightarrow n + f^0$ (1160 MeV < $M_{\pi^+\pi^-}$ < 1380 MeV)

The experimental distributions are compared with that given by the Selleri modification of the Chew Low formula [8] for single pion exchange. (The formula is dependant on the relative angular momentum of the two pions. It is assumed that near the ρ peak the $\pi\pi$ scattering is purely p - wave and near the f^0 purely d - wave). It is seen that the theoretical curve, which has been normalized to the experimental distribution, agrees well with the latter up to $-t \approx 15\,\mu^2$, i.e. over the range where one might expect the Selleri formula to hold. (As a further support of the one pion exchange model we may mention

that the Treiman-Yang angular distribution is isotropic).

Presenting the distribution of the momentum transfer to the proton in a slightly different way reveals an interesting point. From Fig. 4 it may be seen that up to a value of $-t$ equal to $30\mu^2$ the four-momentum transfer distributions for ρ^-, ρ^o and f^o production may all be fitted by an exponential $\frac{d\sigma}{dt} = C\, e^{At}$ with about the same A-value as is obtained from the elastic events. Lines with this A-value are shown in Fig. 4 together with the experimental points. Of course, in the region where the Selleri formula is expected to be applicable the two ways of fitting the data are not really distinguishable.

5. Resonance Production

The effective mass distributions of two-pion systems from reactions (2a) and (2b) (Figs. 5a and 5b), clearly indicate the production of ρ^-, ρ^o and f^o. The presence of these resonant systems can also be seen from the scatter diagrams of $\left(\frac{M_{\pi\pi}}{\mu}\right)^2$ against $\left(\frac{M_{N\pi}}{\mu}\right)^2$ shown in Fig. 6. There is no striking evidence for N^* production, which cannot, of course, result from single pion exchange in these reactions. Fig. 7 shows the same diagrams for events where the four-momentum transfer to the nucleon, $-t$ is less than $15\mu^2$. The presence of the pion resonant systems is here seen more clearly.

From effective mass distributions corresponding to events with all values of t the cross-section for ρ^- production is

found to be (0.45 ± 0.08) mb, and that for ρ^o is found to be (0.75 ± 0.13) mb. The errors quoted allow for uncertainty in subtracting background events. This gives a ratio of 1.67 ± 0.42 for the two cross-sections in agreement with that found in similar experiments [9, 10]. If the ρ is produced exclusively by single pion exchange, charge independence leads to an expected ratio of two.

From Fig. 5 it may be seen that the full width at half height of the ρ^o is about 260 MeV and that of the ρ^- about 180 MeV. These widths are noticeably larger than those reported by other workers, but the discrepancy must be assumed to be real since the experimental errors in the individual mass values are negligible compared with the widths.

The cross-section for the reaction $\pi^- p \longrightarrow n + f^o$ ($f^o \to \pi^+\pi^-$) has a value of (0.42 ± 0.06) mb.

There is no positive evidence for N^* production in the $p\pi^-$, $p\pi^o$ and $n\pi^+$ combinations. The cross-section for the $n\pi^-$ combination is found to be (0.09 ± 0.03) mb.

The total $\pi\pi$ scattering cross-section has been calculated in the ρ and f^o regions using the Selleri formula, restricted to events with $-t \leqslant 15\,\mu^2$. The results are presented in Fig. 8, and are in good agreement with the geometrical cross-sections expected for the ρ and for a spin-two f^o.

Figs. 9 and 10 show scatter diagrams of $\left(\frac{M_{\pi\pi}}{\mu}\right)^2$ versus the angle θ_{π^-} between the incoming and outgoing π^- in the

rest system of the secondary pions. Only events with $-t \leqslant 15\mu^2$ were used. The angle Θ_{π^-} approximately represents the $\pi\pi$ scattering angle. From these figures one obtains in the ρ region a symmetrical angular distribution for ρ^- whereas the ρ^0 yields an asymmetrical distribution as previously reported [10, 11, 12].

In the $\pi^+\pi^-$ effective mass distribution (Fig. 5b) there appears to be a slight excess of events at masses between 760 and 800 MeV which might be attributed to a two pion decay of the ω-meson [13]. Selection of events in different regions of four-momentum transfer shows that these "ω" - events are not preferentially associated with any particular region of momentum transfer.

In I attention was drawn to a peak in the $\pi^+\pi^-$ system at a mass of about 500 MeV arising mainly in the reaction $\pi^- p \longrightarrow p\pi^-\pi^+\pi^-\pi^0$. There is no evidence for such a peaking in the two prong events.

Fig. 11 shows the missing-mass squared distribution for reaction (3a). The peak at $M^2 = 0.31$ GeV^2 presumably arises from neutral η decay and leads to a cross-section of (0.11 ± 0.04) mb for the reaction $\pi^- p \longrightarrow p\pi^-\eta$ if it is assumed that 72% of all η-mesons decay neutrally [14, 15]. This cross-section is compatible with the upper limit of (0.16 ± 0.07) mb given in I.

6. Angular and Momentum Distributions

Fig. 12 shows the centre os mass momentum distributions from reactions (2a) and (2b). Fig. 13 shows the corresponding centre of mass angular distributions.

These distributions clearly reflect the fact that the reactions are dominated by pion resonance production. The sharp peaking of the nucleon momentum distributions indicates the two-body nature of the reactions, while the backward peaking of the nucleon angular distributions arises from the peripheral nature of the interaction.

We have seen above that the π^- from ρ^0 - decay shows a tendency to go forward in the ρ rest system, whereas the ρ^- decays symmetrically. This means that we expect the π^+ in the $n\pi^+\pi^-$ channel to show a greater tendency to go backward in the overall centre of mass system than is the case for the π^0 in the $p\pi^-\pi^0$ channel. This is seen to be the case.

Fig. 14 shows the centre of mass angular distributions of the $\pi\pi$ systems in the mass regions of the ρ and f^0.

For completeness, Figs. 15 and 16 show the centre of mass momentum distributions and Figs. 17 and 18 the centre of mass angular distributions of the charged secondaries from reactions (3a) and (3b).

* * *

Acknowledgements

We are very much indebted to the staff of the CERN proton synchrotron and to the crews of the Saclay 81 cm hydrogen bubble chamber. The help of our scanning teams has been invaluable. Those groups which employ the GRIND fitting programme thank the CERN Data Processing Division.

The groups at Aachen, Bonn and Hamburg are very grateful to the Institut für Plasmaphysik at München-Garching for allowing them the use of their IBM 7090 computer.

The British groups have been supported in part by a grant from the Department of Scientific and Industrial Research. The German groups acknowledge financial support from the Bundesministerium für wissenschaftliche Forschung. Two members of the Munich group (I.D. and N.S.) have been financially supported by the Institut fur theoretische Physik der Universität München.

* * *

References:

1. Aachen - Birmingham - Bonn - Hamburg - London (I.C.) - Munchen collaboration: Nuovo Cimento to be published.
2. C. C. Ting, L. W. Jones, M. L. Perl: Phys. Rev. Lett., 9, 468 (1962).
3. S. Brandt, V. T. Cocconi, D. R. C. Morrison, A. Wroblewski, P. Fleury, G. Kayas, F. Muller, C. Pelletier: Phys. Rev. Lett., 10, 413 (1963).
4. S. J. Lindenbaum, W. A. Love, J. A. Niederer, S. Ozaki, J. J. Russel, L. C. L. Yuan: Phys. Rev. Lett., 7, 352 (1961).
5. G. von Dardel, D. Dekkers, R. Mermond, M. Vivargent, G. Weber, K. Winter: Phys. Rev. Lett., 8, 173 (1962).
6. A. N. Diddens, E. W. Jenkins, T. F. Kycia, K. F. Riley: Phys. Rev. Lett. 10, 262 (1963).
7. Aachen - Birmingham - Bonn - Hamburg - London (i.C.) - Munchen collaboration: Phys. Lett., 5, 153 (1963).
8. F. Selleri: Phys. Lett., 3, 76 (1962).
9. E. Pickup, D. K. Robinson, E. O. Salant: Phys. Rev. Lett., 7, 192 (1961).
10. Saclay - Orsay - Bari - Bologna collaboration: Nuovo Cimento to be published.
11. G. Puppi: Proc. of the 1962 International Conference on High-Energy Physics at CERN, p. 713 (1962).
12. W. Selove, V. Hagopian, H. Brody, A. Baker, E. Leboy: Phys. Rev. Lett., 9, 272 (1962).
13. W. J. Fickinger, D. K. Robinson, E. O. Salant: Phys. Rev. Lett., 10, 457 (1963).
14. C. Alff, D. Berley, D. Colley, N. Gelfand, U. Nauenberg, D. Miller, J. Schultz, J. Steinberger, T. H. Tan, H. Brugger, P. Kramer, R. Plane: Phys. Rev. Lett., 9, 325 (1962).
15. M. Meer, R. Strand, R. Kraemer, L. Mandansky, M. Nussbaum, A. Pevsner, C. Richardson, T. Toohig, M. Block, S. Orenstein, T. Fields: Proc. of the 1962 International Conference on High Energy Physics at CERN, p. 103 (1962).

* * *

Figure Captions

Fig. 1: Differential cross-section, for elastic scattering.
a) for all values of four-momentum transfer
b) for $-t \leqslant 0.6$ GeV^2
The solid line shows the fit $(52.87 \pm 3.96) \exp (8.53 \pm 0.49)\, t$.

Fig. 2: One pion exchange diagram.

Fig. 3: Distribution of four-momentum transfer to the nucleon:
a) for reaction $\pi^- p \rightarrow p + \rho^-$
b) for reaction $\pi^- p \rightarrow n + \rho^0$
c) for reaction $\pi^- p \rightarrow n + f^0$
The solid line shows the prediction of the Selleri formula.
Only events with $-t \leqslant 30\ \mu^2$ are included.

Fig. 4: Distribution of four-momentum transfer to the nucleon in the reactions:
The solid lines show $\partial\sigma/\partial t = A \exp (8.53\, t)$.

Fig. 5: Effective mass distributions of $\pi\pi$ system:
a) reaction $\pi^- p \rightarrow p\, \pi^- \pi^0$
b) reaction $\pi^- p \rightarrow n\, \pi^+ \pi^-$
Phase space curves normalized to events outside ρ and f^0 peaks.

Fig. 6: Scatter diagram of $\left(\frac{M_{\pi\pi}}{\mu}\right)^2$ against $\left(\frac{M_{N\pi}}{\mu}\right)^2$:
a) for reaction $\pi^- p \rightarrow p\, \pi^- \pi^0$
b) for reaction $\pi^- p \rightarrow n\, \pi^+ \pi^-$
The dotted lines indicate the isobar bands.

Fig. 7: Scatter diagram of $\left(\frac{M_{\pi\pi}}{\mu}\right)^2$ against $\left(\frac{M_{\pi N}}{\mu}\right)^2$ for events with $-t \leqslant 15\ \mu^2$:
a) for reaction $\pi^- p \rightarrow p\, \pi^- \pi^0$
b) for reaction $\pi^- p \rightarrow n\, \pi^+ \pi^-$
The boundary curves are those arising when there is no limitation on t.

Fig. 8: Cross-section for $\pi\pi$ scattering:
a) from the reaction $\pi^- p \rightarrow p\,\pi^-\,\pi^0$ in the ρ region
b) from the reaction $\pi^- p \rightarrow n\,\pi^+\,\pi^-$ in the ρ region
c) from the reaction $\pi^- p \rightarrow n\,\pi^+\,\pi^-$ in the f^0 region

Fig. 9: Scatter diagram of $\left(\frac{M_{\pi^-\pi^0}}{\mu}\right)^2$ versus the angle between the incoming and outgoing π^- in the $\pi^-\,\pi^0$ rest system for $-t \leqslant 15\mu^2$.

Fig. 10: Scatter diagram of $\left(\frac{M_{\pi^+\pi^-}}{\mu}\right)^2$ versus the angle between the incoming and outgoing π^- in the $\pi^+\,\pi^-$ rest system for $-t \leqslant 15\,\mu^2$.

Fig. 11: Missing mass squared distribution for the reaction $\pi^- p \rightarrow p\,\pi^-\,(m\,\pi^0)$, $m \geqslant 2$.

Fig. 12: Centre of mass momentum distributions for reactions $\pi^- p \rightarrow p\,\pi^-\,\pi^0$ (2a) and $\pi^- p \rightarrow n\,\pi^+\,\pi^-$ (2b):
a) proton from reaction (2a)
b) π^- from reaction (2a)
c) π^0 from reaction (2a)
d) neutron from reaction (2b)
e) π^- from reaction (2b)
f) π^+ from reaction (2b)

Fig. 13: Centre of mass angular distributions for reactions $\pi^- p \rightarrow p\,\pi^-\,\pi^0$ (2a) and $\pi^- p \rightarrow n\,\pi^+\,\pi^-$ (2b):
a) proton from reaction (2a)
b) π^- from reaction (2a)
c) π^0 from reaction (2a)
d) neutron from reaction (2b)
e) π^- from reaction (2b)
f) π^+ from reaction (2b)

Fig. 14: Centre of mass angular distributions of $\pi\pi$ systems:
a) In the ρ^- region of reaction $\pi^- p \rightarrow p\,\pi^-\,\pi^0$
b) In the ρ^0 region of reaction $\pi^- p \rightarrow n\,\pi^+\,\pi^-$
c) In the f^0 region of reaction $\pi^- p \rightarrow n\,\pi^+\,\pi^-$

Fig. 15: Centre of mass momentum distributions for the reaction $\pi^- p \longrightarrow p \pi^- (m \pi^0)$, $m \geq 2$:
a) proton
b) π^-

Fig. 16: Centre of mass momentum distributions for the reaction $\pi^- p \longrightarrow n \pi^+ \pi^- (m \pi^0)$, $m \geq 1$:
a) π^+
b) π^-

Fig. 17: Centre of mass angular distributions for the reaction $\pi^- p \longrightarrow p \pi^- (m \pi^0)$, $m \geq 2$:
a) proton
b) π^-

Fig. 18: Centre of mass angular distributions for the reaction $\pi^- p \longrightarrow n \pi^+ \pi^- (m \pi^0)$, $m \geq 1$:
a) π^+
b) π^-

* * *

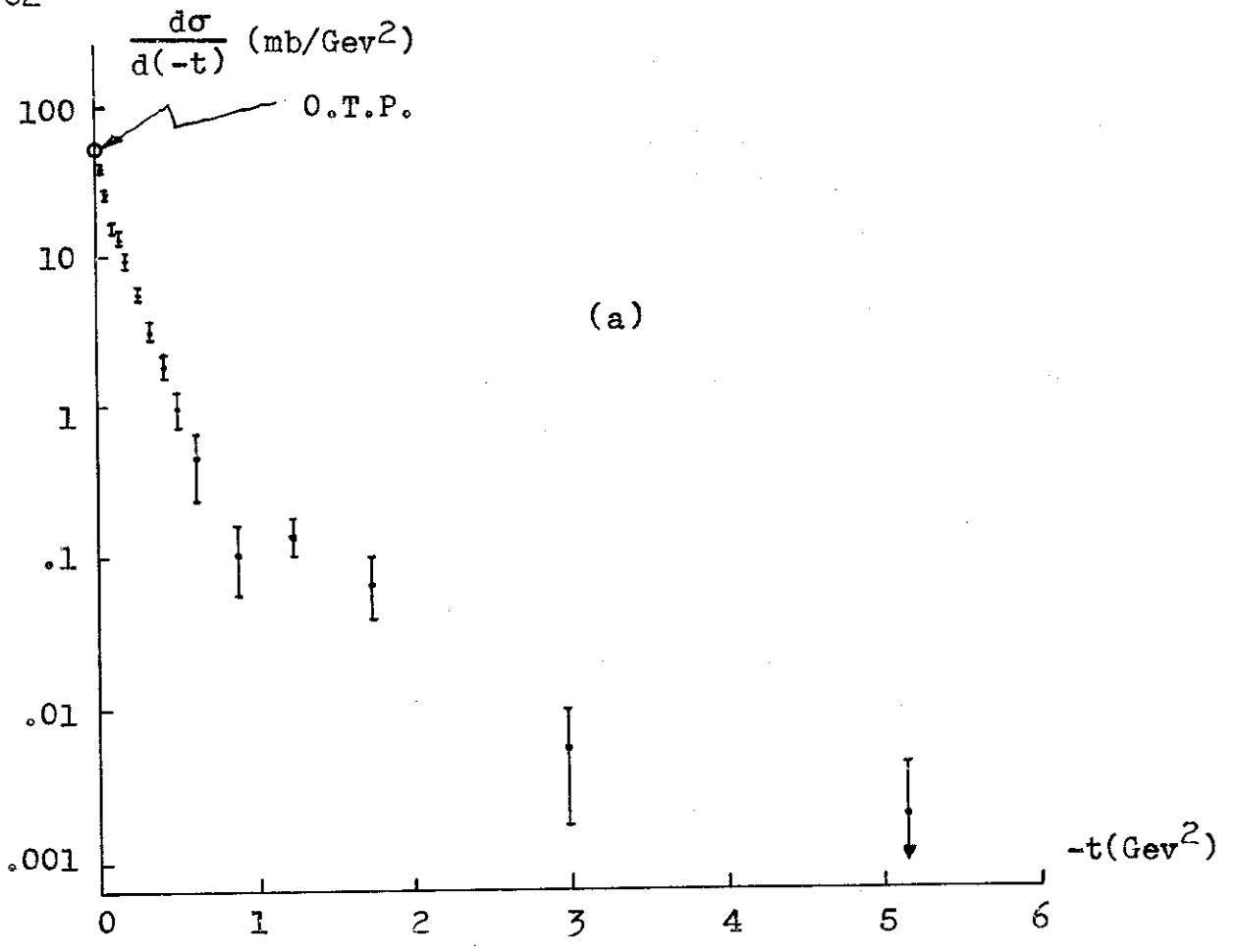
dσ/d(-t) (mb/Gev²)
O.T.P.
(a)
100
10
1
.1
.01
.001
-t(Gev²)
0
1
2
3
4
5
6

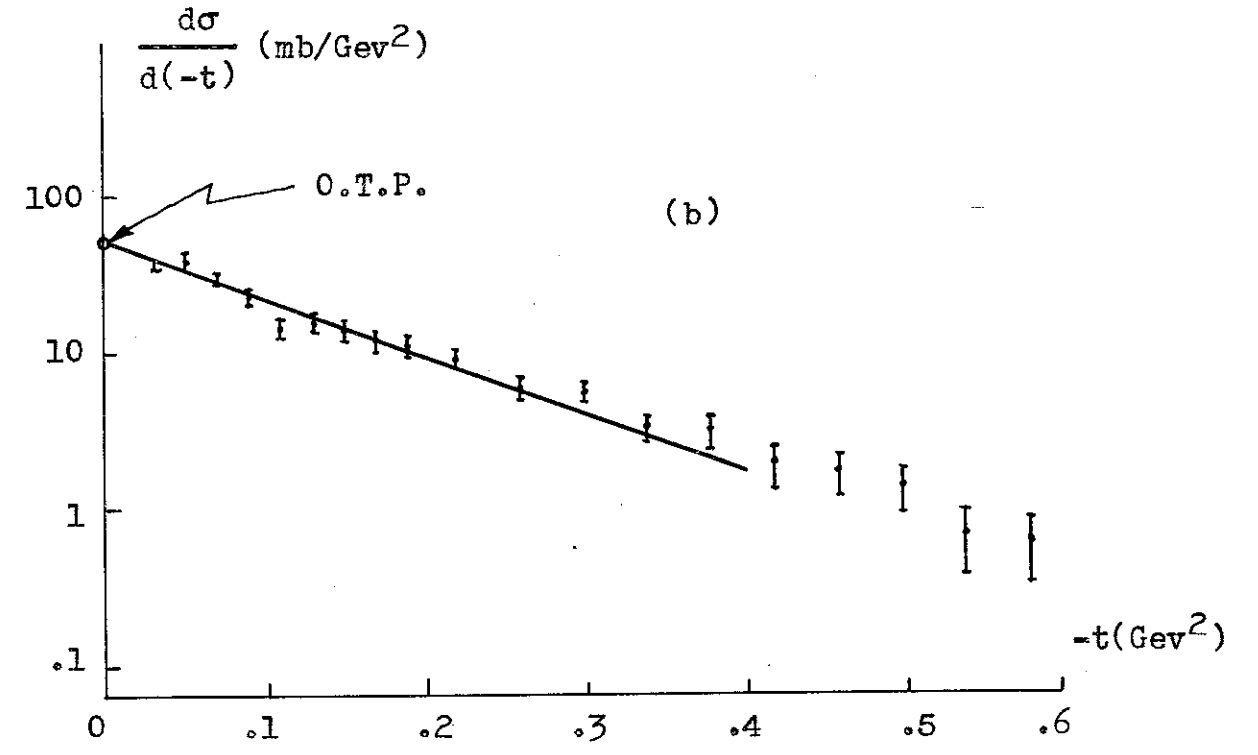
dσ/d(-t) (mb/Gev²)
O.T.P.
(b)
100
10
1
.1
-t(Gev²)
0
.1
.2
.3
.4
.5
.6

FIG. 1

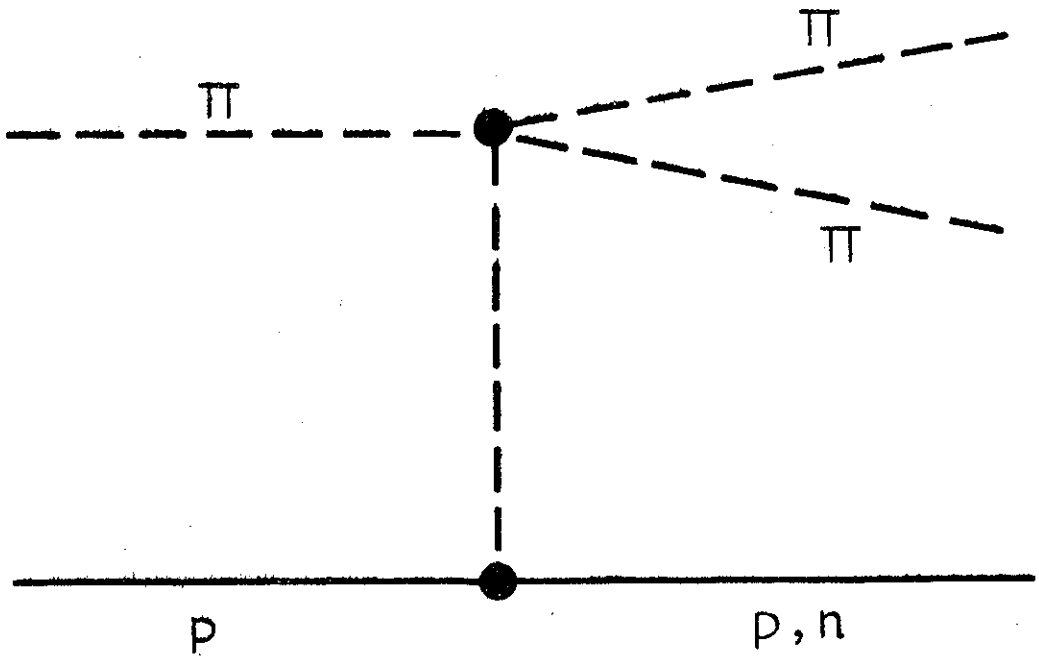

FIG. 2

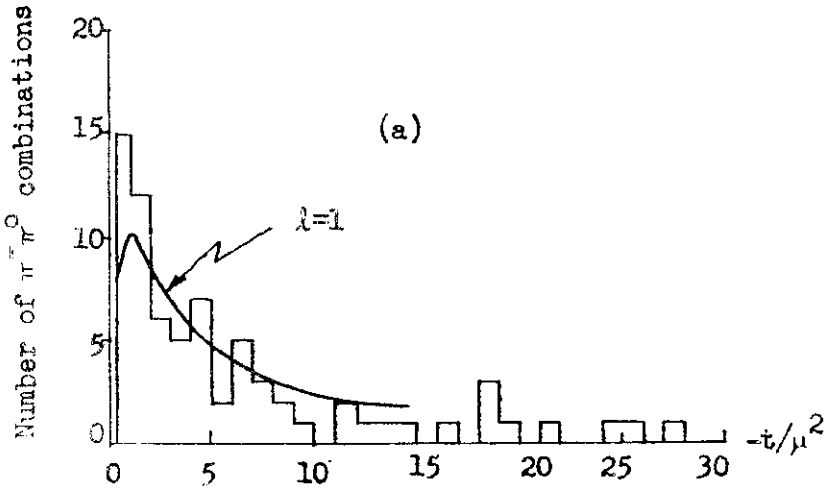
Number of $\pi^- \pi^0$ combinations
(a)
λ=1
$-t/\mu^2$

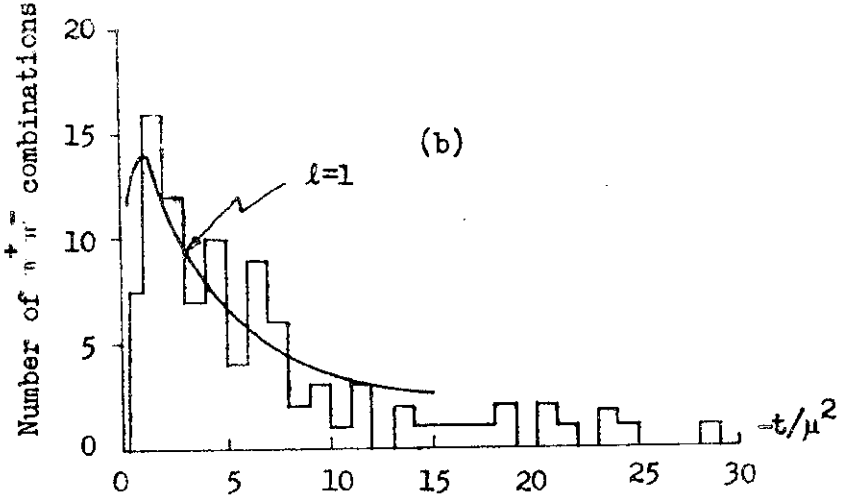
Number of $\pi^+ \pi^-$ combinations
(b)
ℓ=1
$-t/\mu^2$

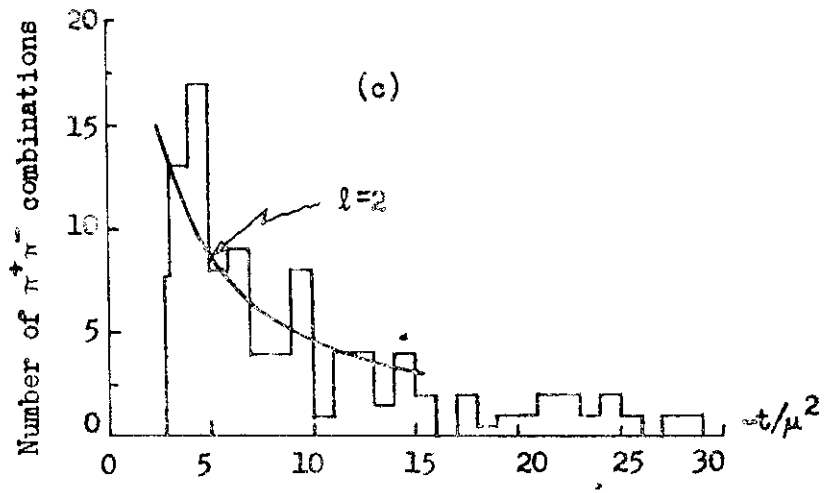
Number of $\pi^+ \pi^-$ combinations
(c)
ℓ=2
$-t/\mu^2$

FIG. 3

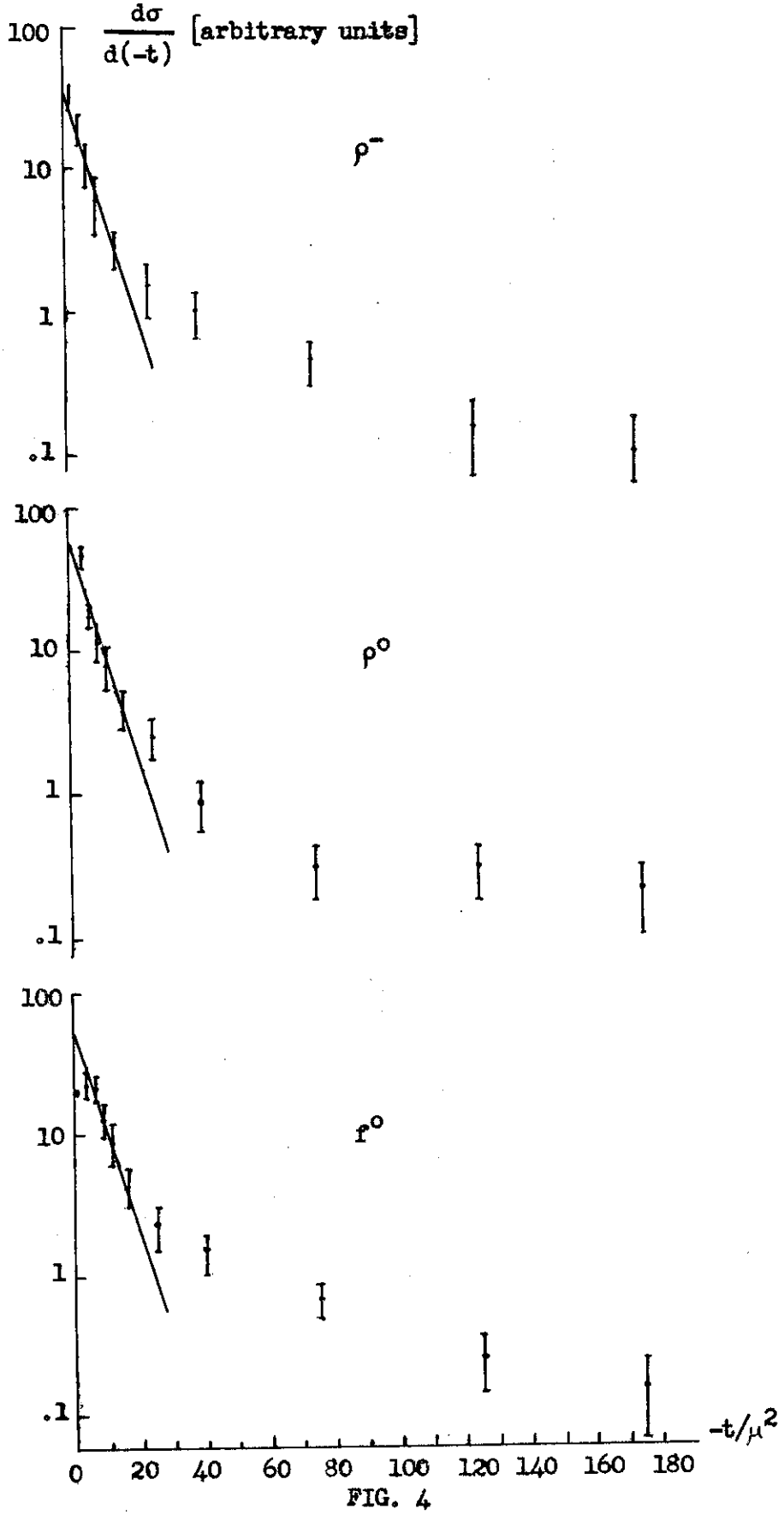
dσ/d(-t) [arbitrary units]
100
10
1
.1
ρ⁻
ρ°
f°
-t/μ²
0
20
40
60
80
100
120
140
160
180

FIG. 4

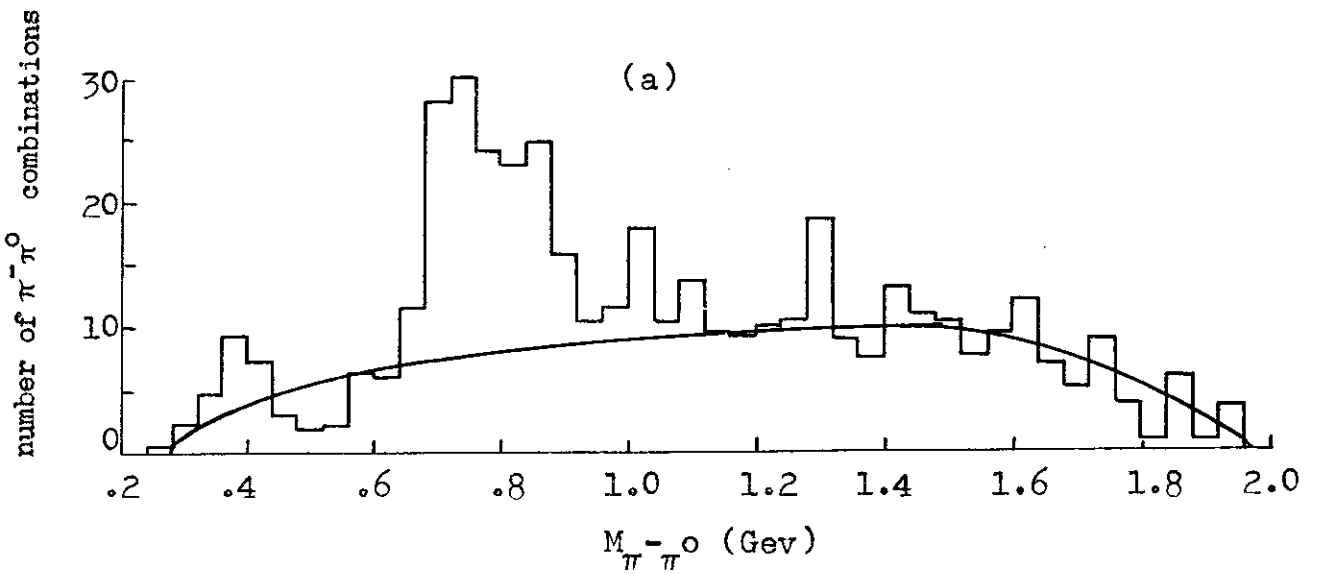
(a)
number of $\pi^-\pi^0$ combinations
30
20
10
0
.2
.4
.6
.8
1.0
1.2
1.4
1.6
1.8
2.0
$M_{\pi^-\pi^0}$ (Gev)

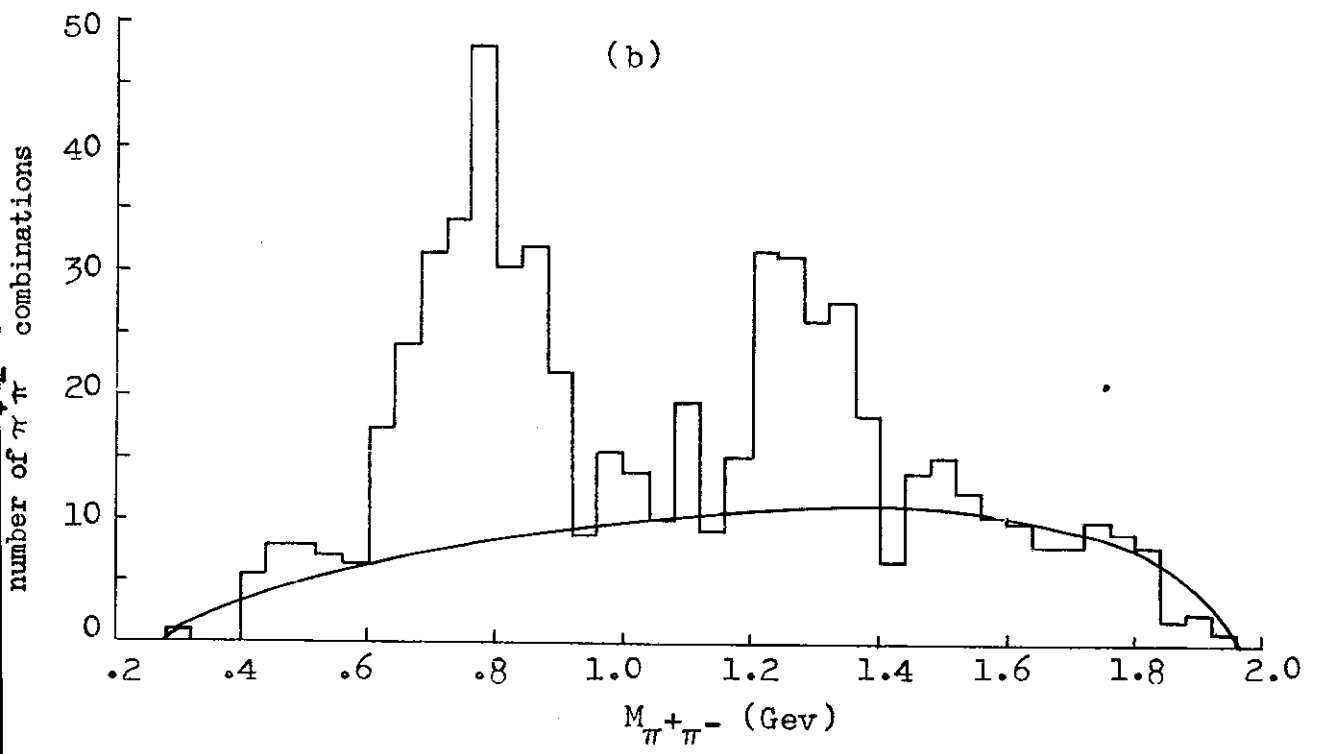
(b)
number of $\pi^+\pi^-$ combinations
50
40
30
20
10
0
.2
.4
.6
.8
1.0
1.2
1.4
1.6
1.8
2.0
$M_{\pi^+\pi^-}$ (Gev)

FIG. 5

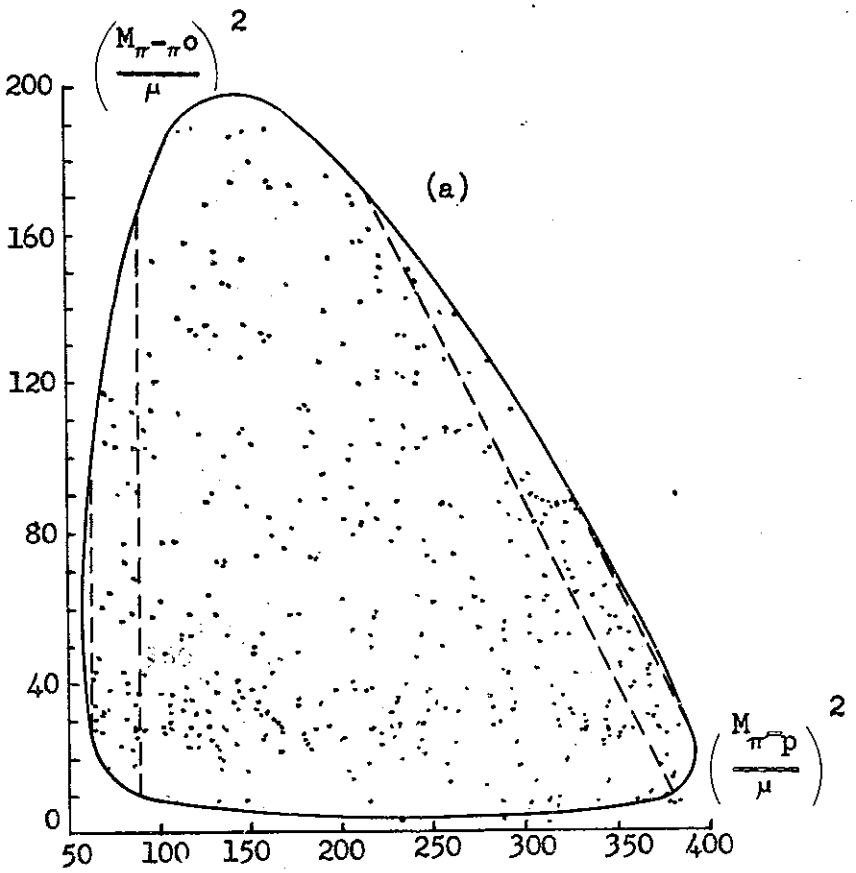
$\left(\frac{M_{\pi^-\pi^0}}{\mu}\right)^2$
200
160
120
80
40
0
(a)
50
100
150
200
250
300
350
400
$\left(\frac{M_{\pi^-p}}{\mu}\right)^2$

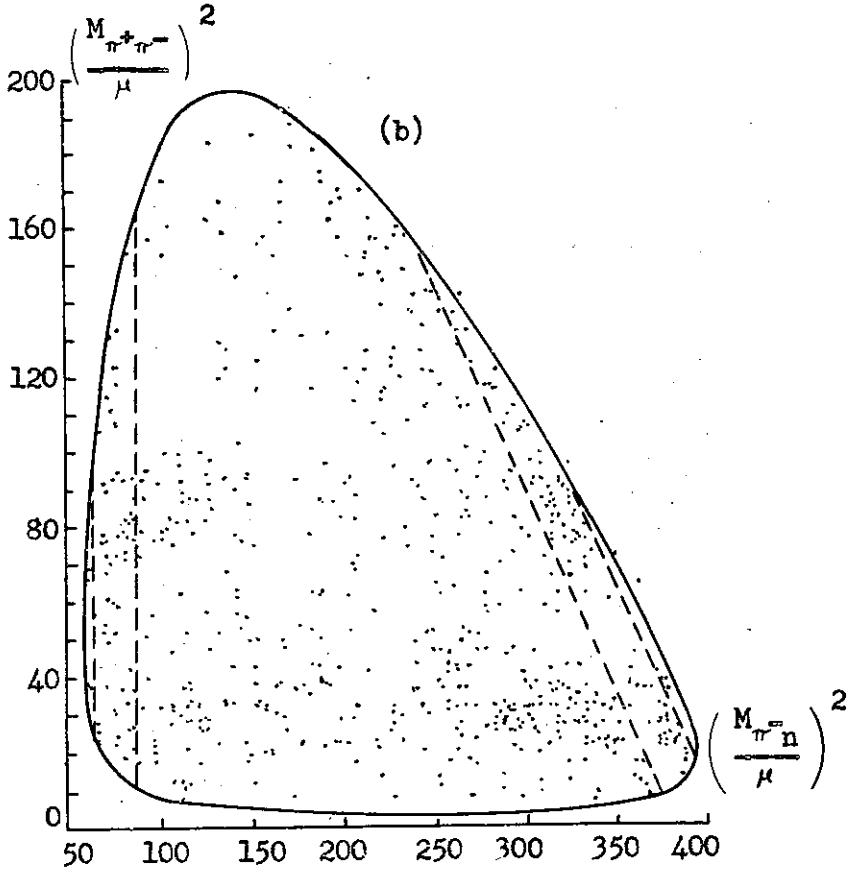
$\left(\frac{M_{\pi^+\pi^-}}{\mu}\right)^2$
200
160
120
80
40
0
(b)
50
100
150
200
250
300
350
400
$\left(\frac{M_{\pi^-n}}{\mu}\right)^2$

FIG. 6

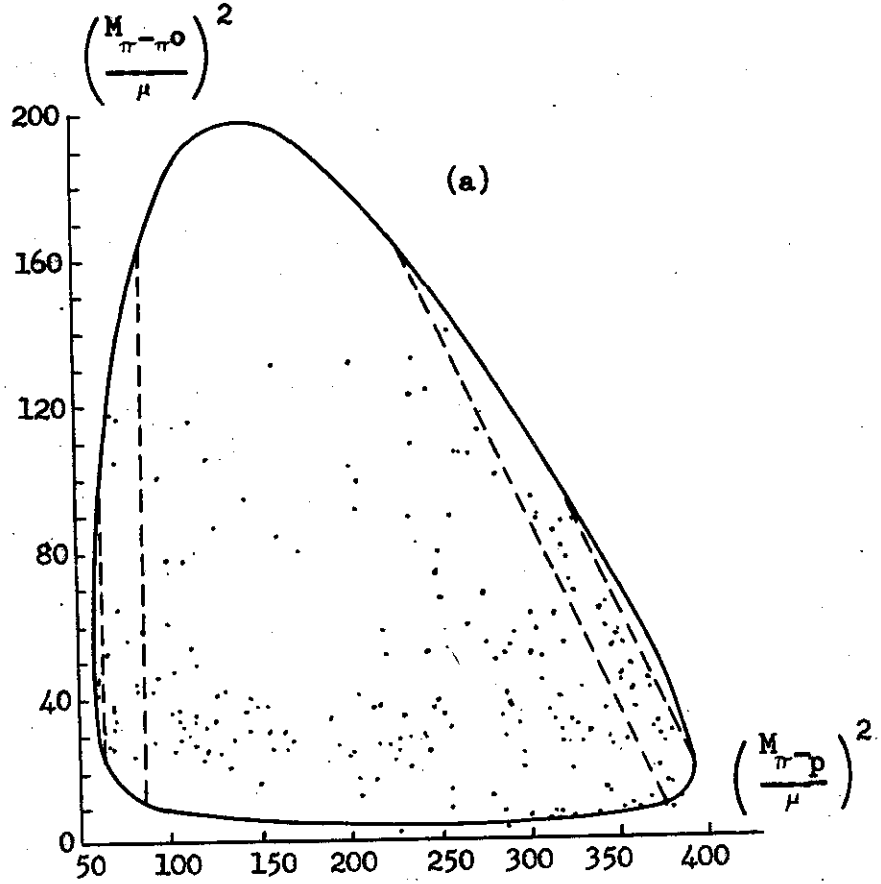
$\left(\frac{M_{\pi^-\pi^0}}{\mu}\right)^2$
200
160
120
80
40
0
(a)
50
100
150
200
250
300
350
400
$\left(\frac{M_{\pi^-p}}{\mu}\right)^2$

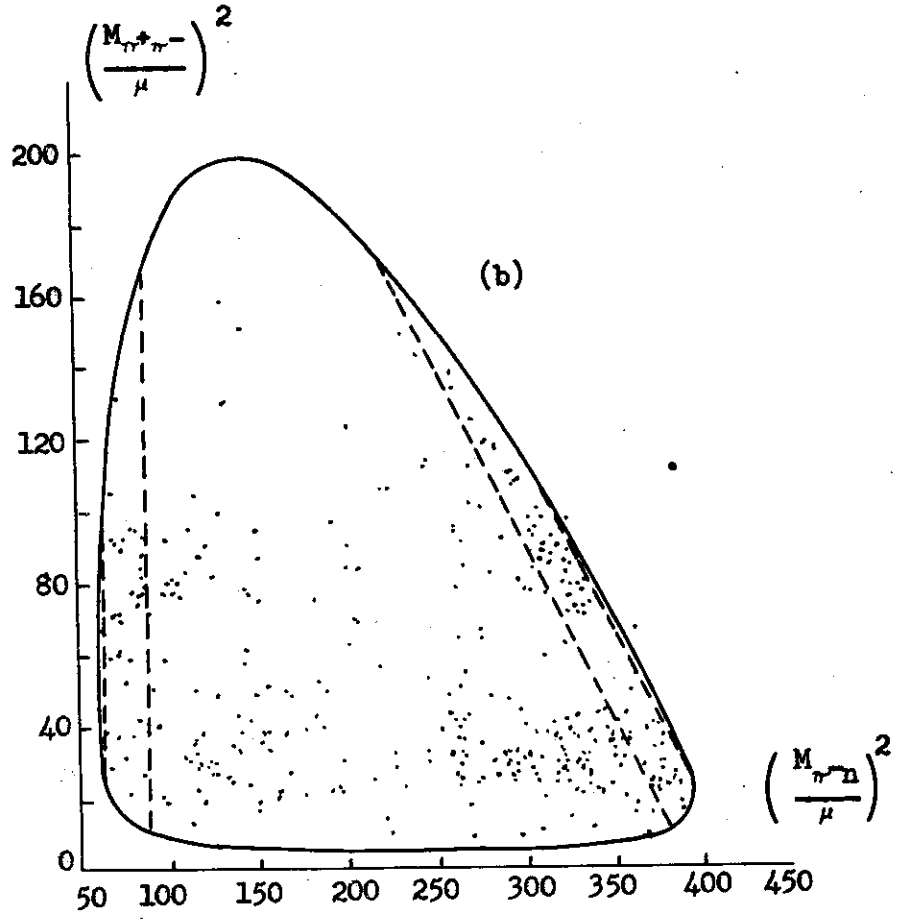
$\left(\frac{M_{\pi^+\pi^-}}{\mu}\right)^2$
200
160
120
80
40
0
(b)
50
100
150
200
250
300
350
400
450
$\left(\frac{M_{\pi^-n}}{\mu}\right)^2$

FIG. 7

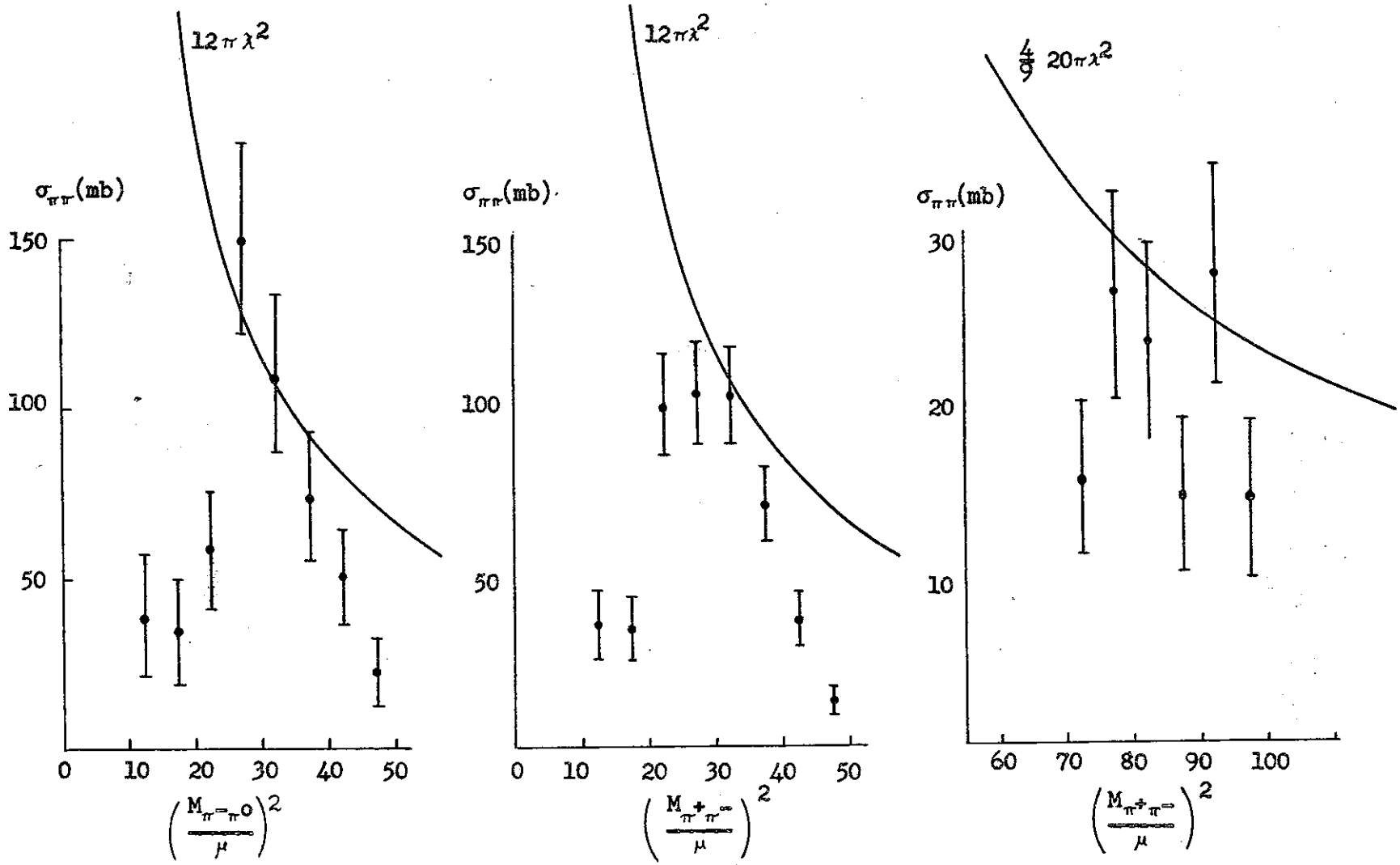
$12\pi\lambda^2$
$\sigma_{\pi\pi}$(mb)
150
100
50
0
10
20
30
40
50
$\left(\frac{M_{\pi^-\pi^0}}{\mu}\right)^2$
(a)
$12\pi\lambda^2$
$\sigma_{\pi\pi}$(mb)
150
100
50
0
10
20
30
40
50
$\left(\frac{M_{\pi^+\pi^-}}{\mu}\right)^2$
(b)
$\frac{4}{9}\ 20\pi\lambda^2$
$\sigma_{\pi\pi}$(mb)
30
20
10
60
70
80
90
100
$\left(\frac{M_{\pi^+\pi^-}}{\mu}\right)^2$
(c)

FIG. 8

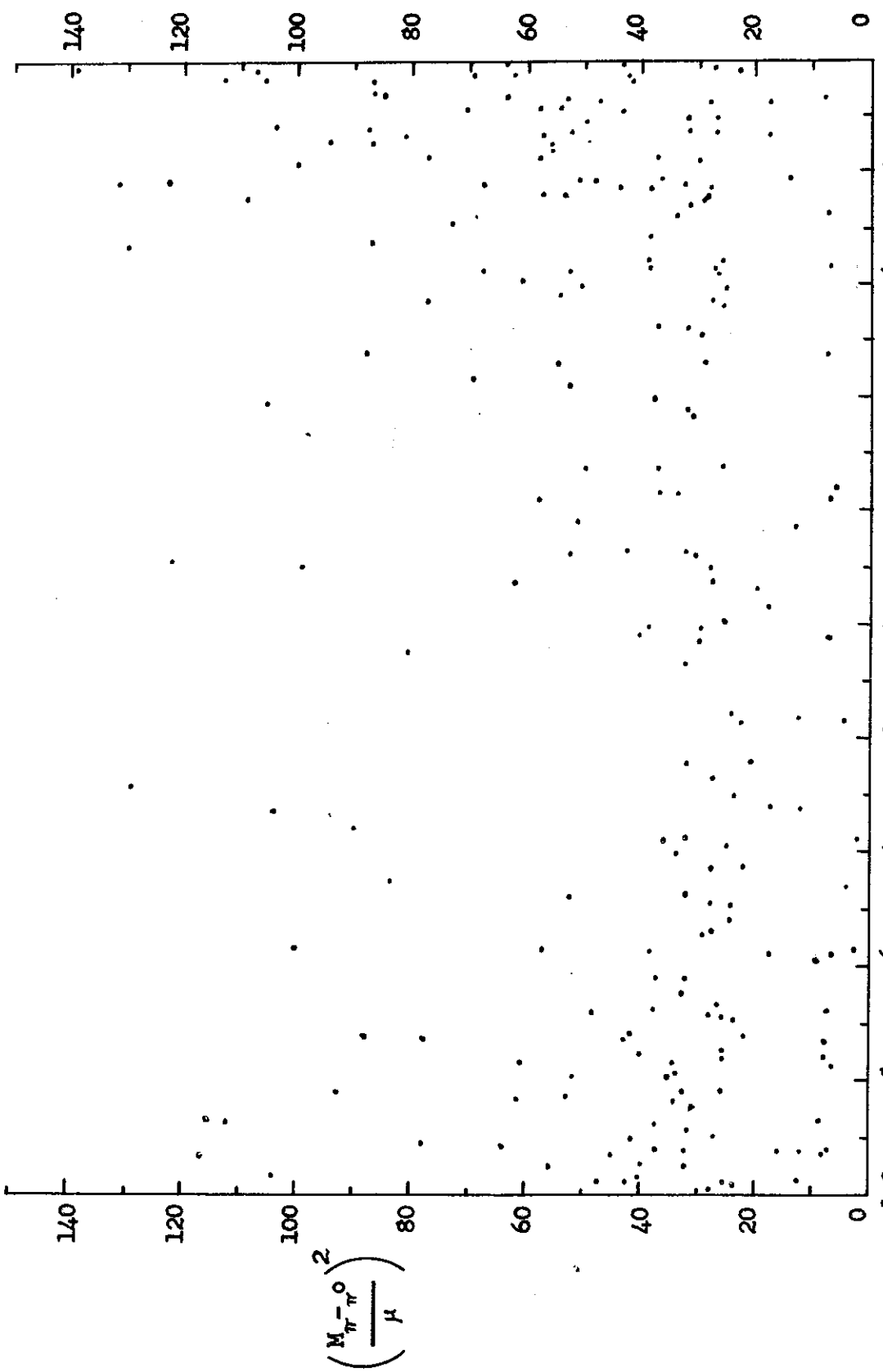
$\left(\frac{M_{\pi^-\pi^0}}{\mu}\right)^2$
0
20
40
60
80
100
120
140
-1.0
-.8
-.6
-.4
-.2
0
.2
.4
.6
.8
1.0
$\cos\theta_{\pi^-}$

FIG. 9

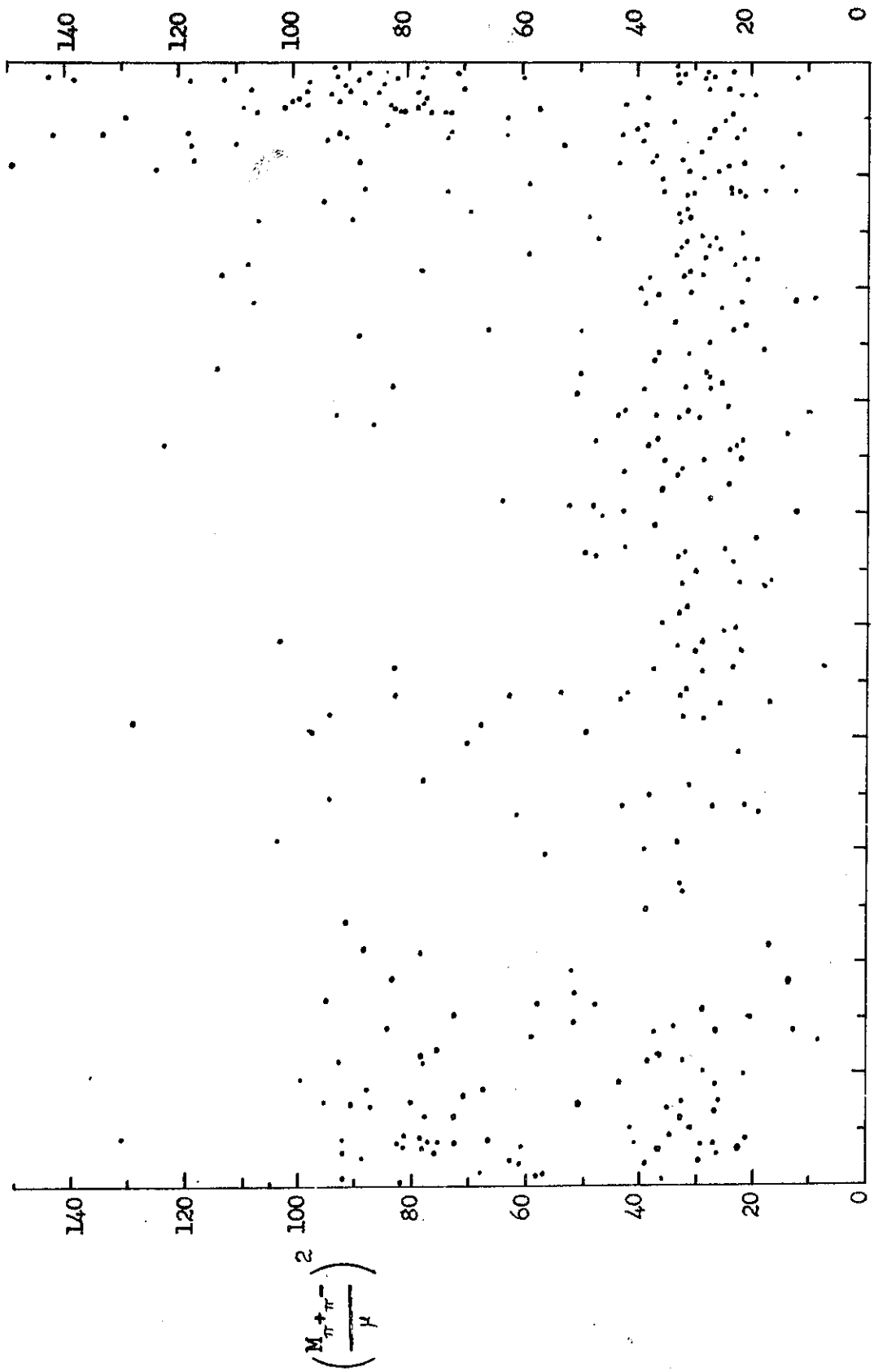
$\left(\frac{M_{\pi^+\pi^-}}{\mu}\right)^2$
140
120
100
80
60
40
20
0
-1.0
-.8
-.6
-.4
-.2
0
.2
.4
.6
.8
1.0
$\cos\theta_{\pi^-}$

FIG. 10

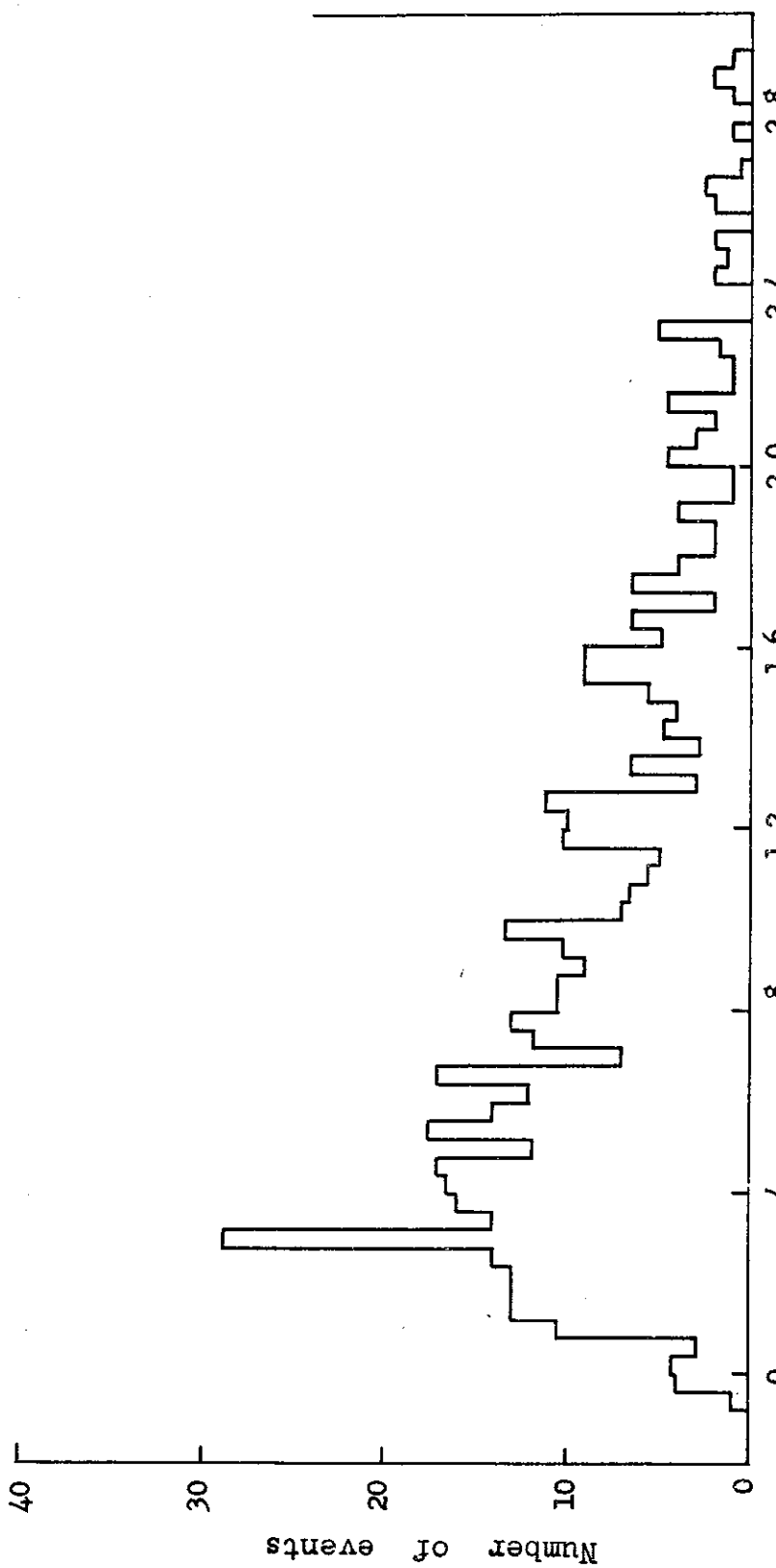
Number of events
40
30
20
10
0
0
.4
.8
1.2
1.6
2.0
2.4
2.8
(missing mass)^2 Gev^2

FIG. 11

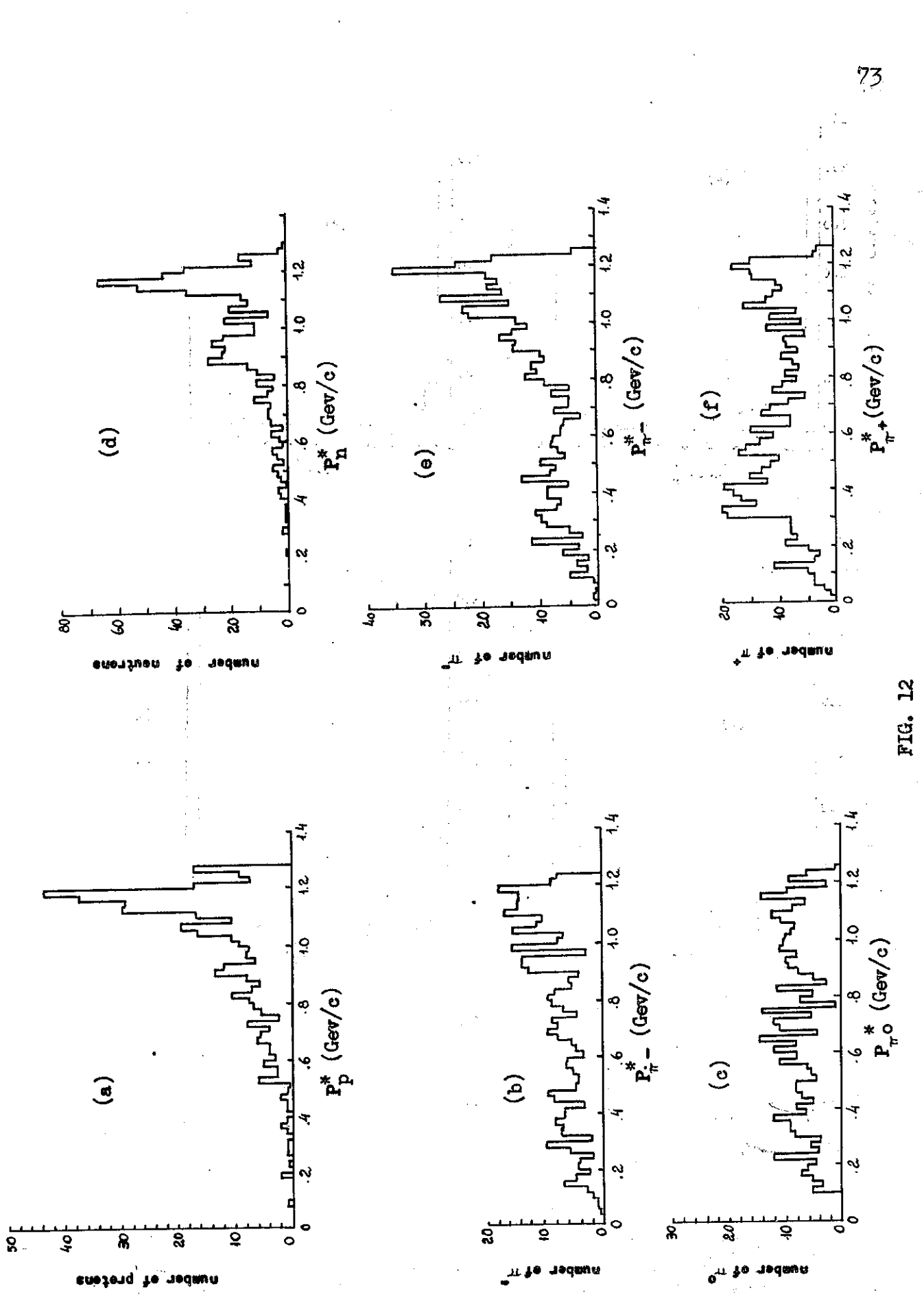
(a)
number of protons
P_p^* (Gev/c)
(b)
number of π^-
$P_{\pi^-}^*$ (Gev/c)
(c)
number of π^0
$P_{\pi^0}^*$ (Gev/c)
(d)
number of neutrons
P_n^* (Gev/c)
(e)
number of π^-
$P_{\pi^-}^*$ (Gev/c)
(f)
number of π^+
$P_{\pi^+}^*$ (Gev/c)

FIG. 12

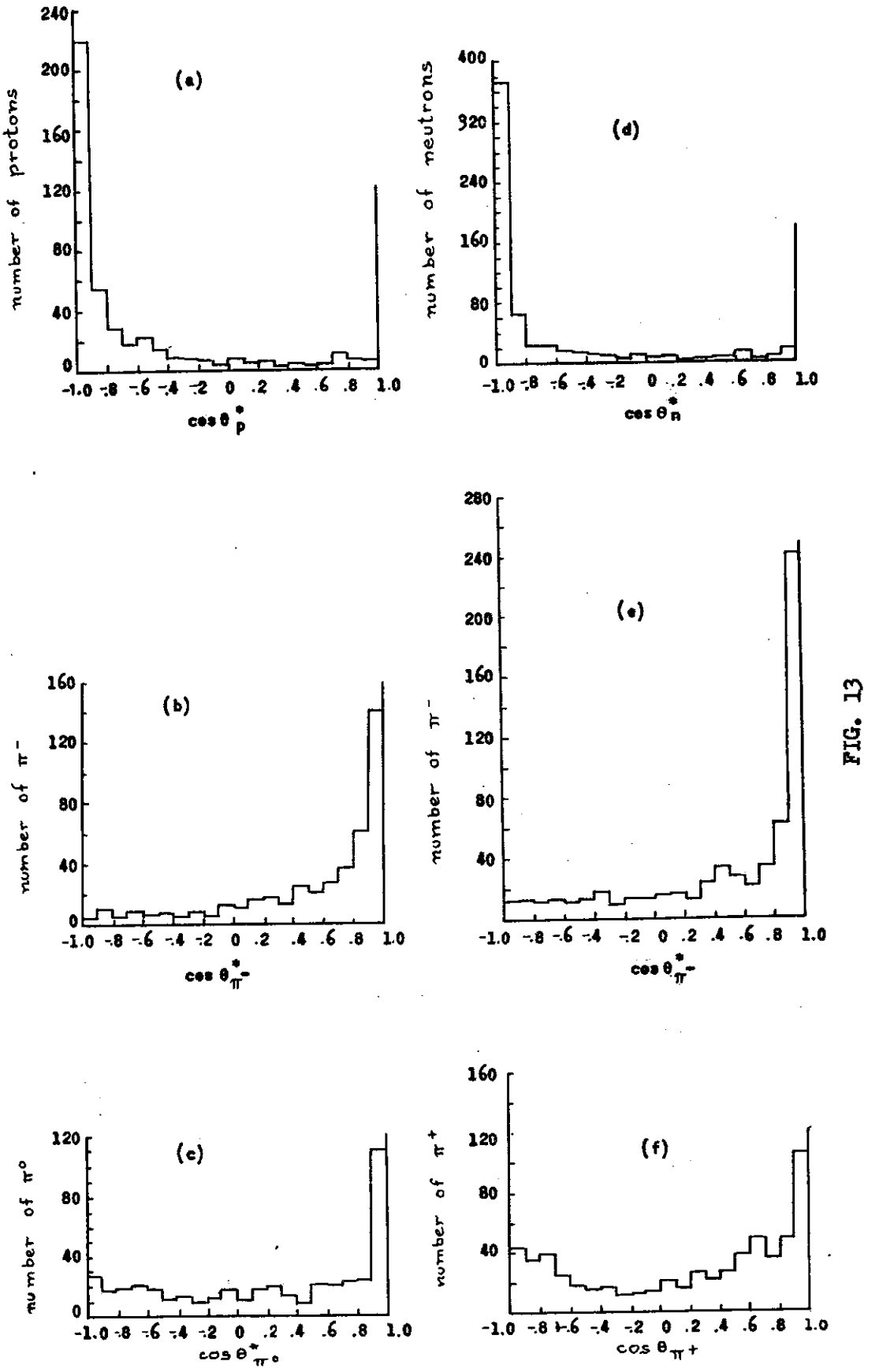
(a)
number of protons
240
200
160
120
80
40
0
-1.0 -.8 -.6 -.4 -.2 0 .2 .4 .6 .8 1.0
cos θ*p
(d)
number of neutrons
400
320
240
160
80
0
-1.0 -.8 -.6 -.4 -.2 0 .2 .4 .6 .8 1.0
cos θ*n
(b)
number of π⁻
160
120
80
40
0
-1.0 -.8 -.6 -.4 -.2 0 .2 .4 .6 .8 1.0
cos θ*π⁻
(e)
number of π⁻
280
240
200
160
120
80
40
-1.0 -.8 -.6 -.4 -.2 0 .2 .4 .6 .8 1.0
cos θ*π⁻
(c)
number of π°
120
80
40
0
-1.0 -.8 -.6 -.4 -.2 0 .2 .4 .6 .8 1.0
cos θ*π°
(f)
number of π⁺
160
120
80
40
-1.0 -.8 -.6 -.4 -.2 0 .2 .4 .6 .8 1.0
cos θπ⁺

FIG. 13

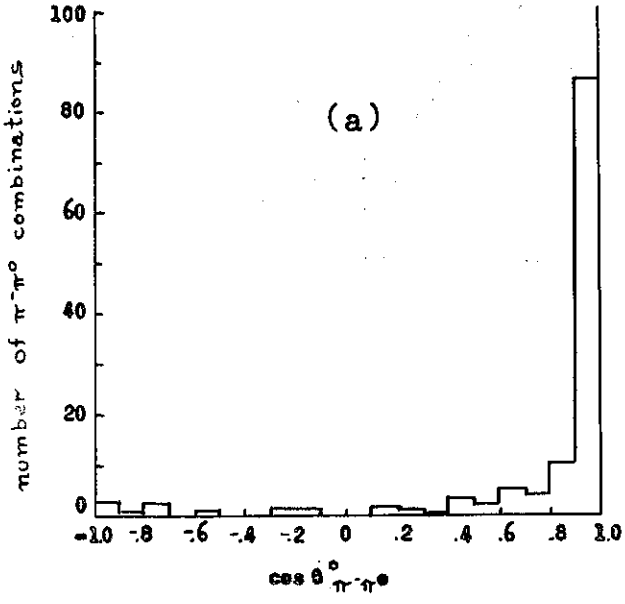
(a)
number of $\pi^-\pi^0$ combinations
100
80
60
40
20
0
-1.0 -.8 -.6 -.4 -.2 0 .2 .4 .6 .8 1.0
$\cos\theta^*_{\pi^-\pi^0}$

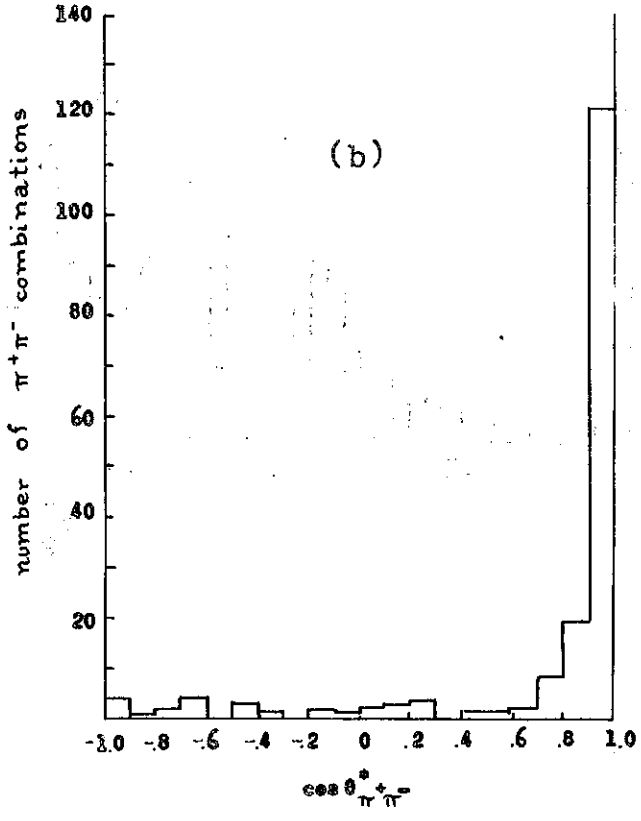
(b)
number of $\pi^+\pi^-$ combinations
140
120
100
80
60
40
20
-1.0 -.8 -.6 -.4 -.2 0 .2 .4 .6 .8 1.0
$\cos\theta^*_{\pi^+\pi^-}$

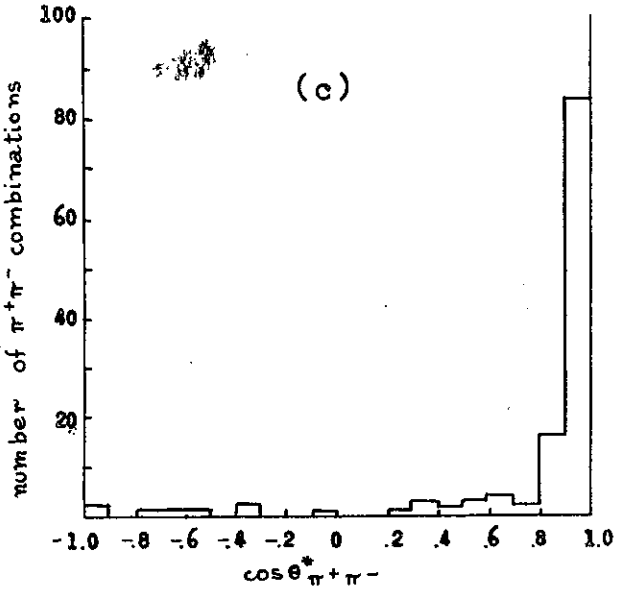
(c)
number of $\pi^+\pi^-$ combinations
100
80
60
40
20
-1.0 -.8 -.6 -.4 -.2 0 .2 .4 .6 .8 1.0
$\cos\theta^*_{\pi^+\pi^-}$

FIG. 14

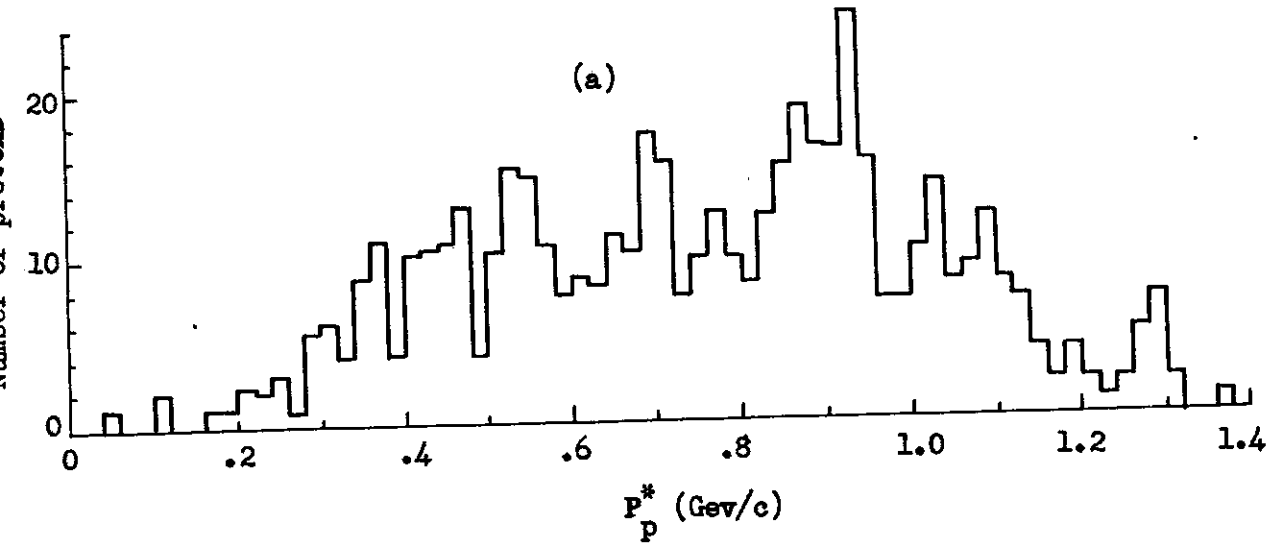
(a)
20
10
0
0
.2
.4
.6
.8
1.0
1.2
1.4
P_p^* (Gev/c)

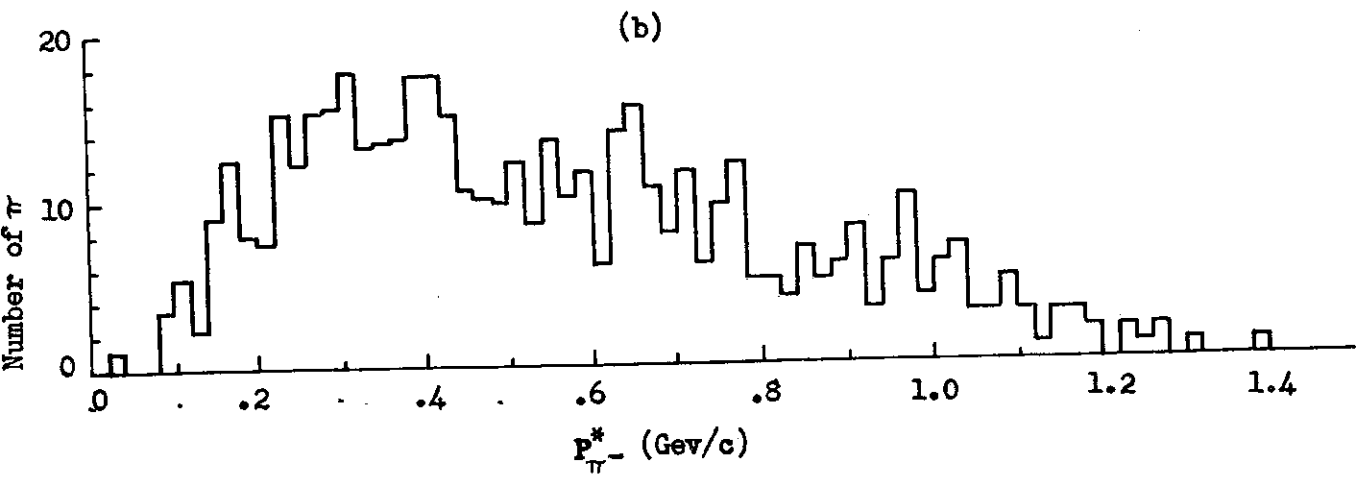
(b)
20
10
0
Number of π^-
0
.2
.4
.6
.8
1.0
1.2
1.4
$P_{\pi^-}^*$ (Gev/c)

FIG. 15

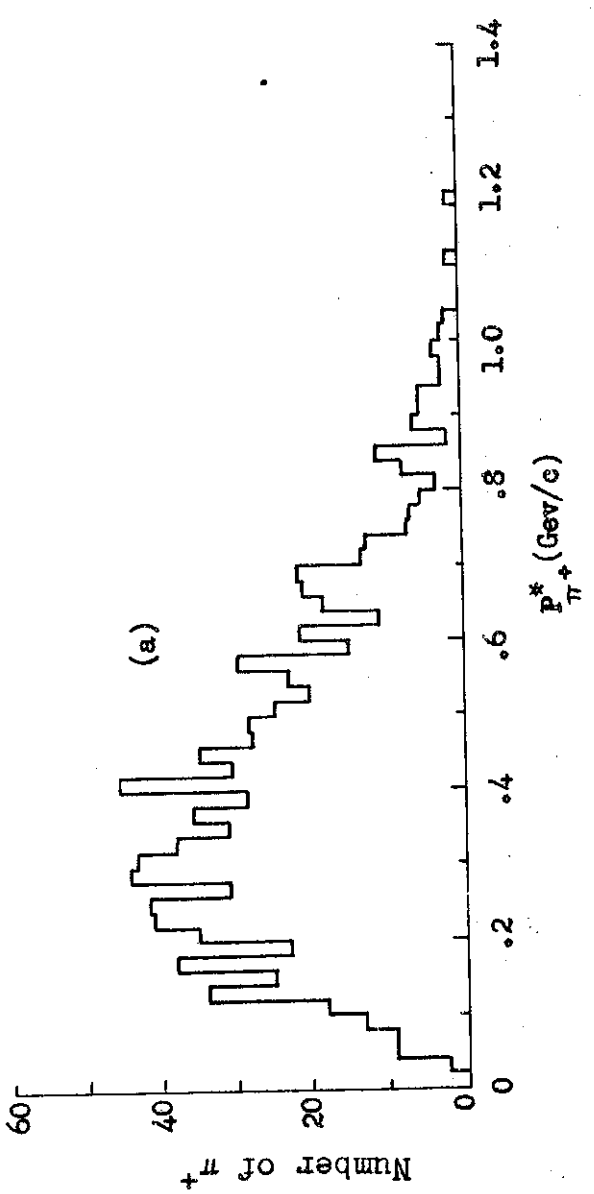
(a)
Number of π^+
0
20
40
60
0
.2
.4
.6
.8
1.0
1.2
1.4
$P^*_{\pi^+}$ (Gev/c)

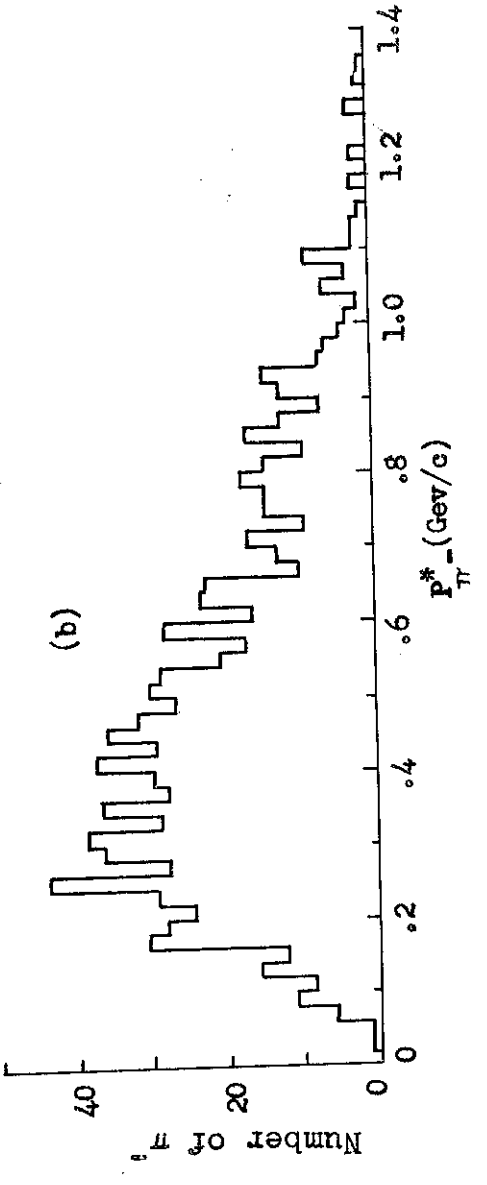
(b)
Number of π^-
0
20
40
0
.2
.4
.6
.8
1.0
1.2
1.4
$P^*_{\pi^-}$ (Gev/c)

FIG. 16

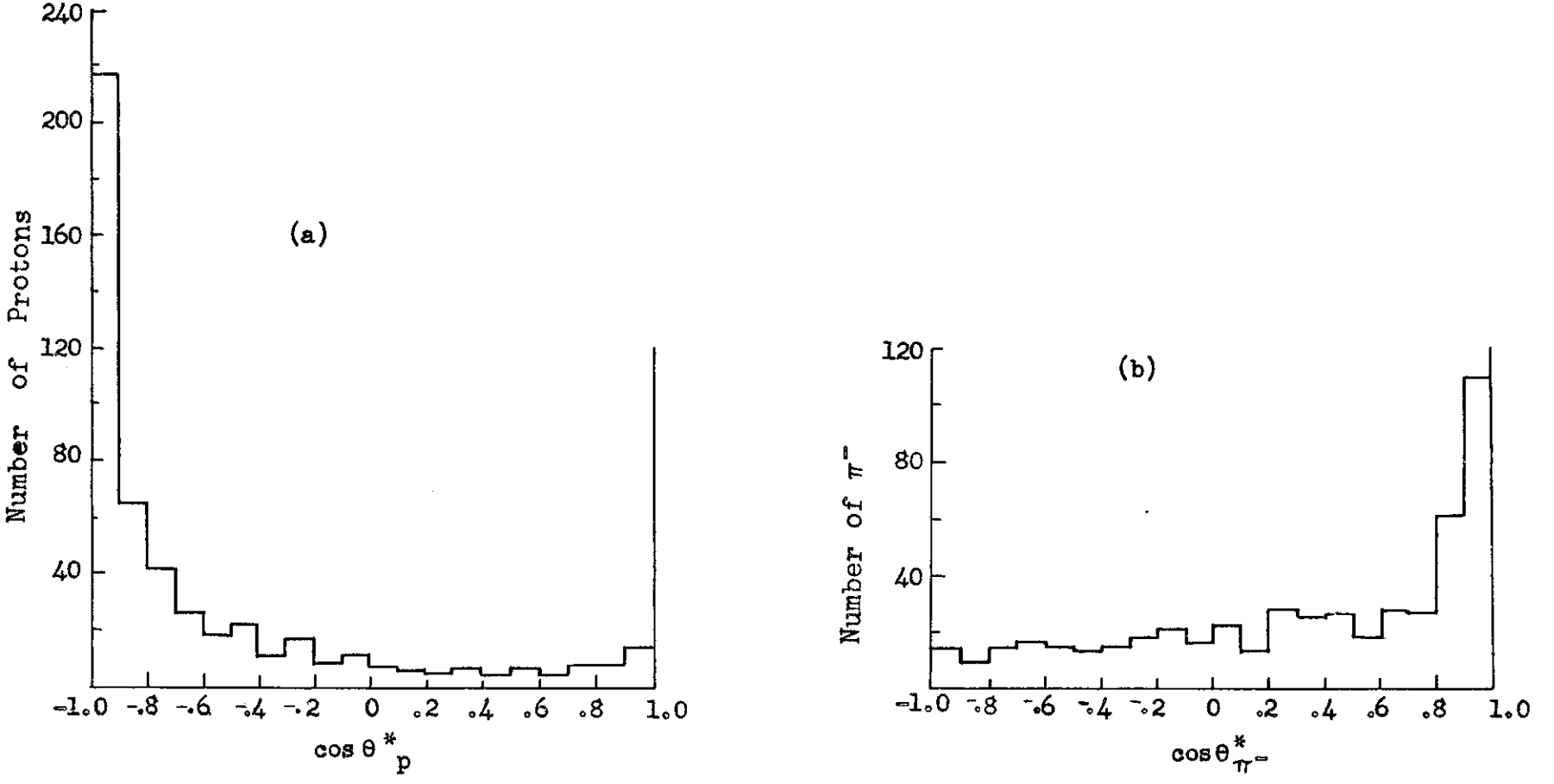
240
200
160
120
80
40
Number of Protons
(a)
-1.0 -.8 -.6 -.4 -.2 0 .2 .4 .6 .8 1.0
cos θ* p
120
80
40
Number of π⁻
(b)
-1.0 -.8 -.6 -.4 -.2 0 .2 .4 .6 .8 1.0
cos θ* π⁻

FIG. 17

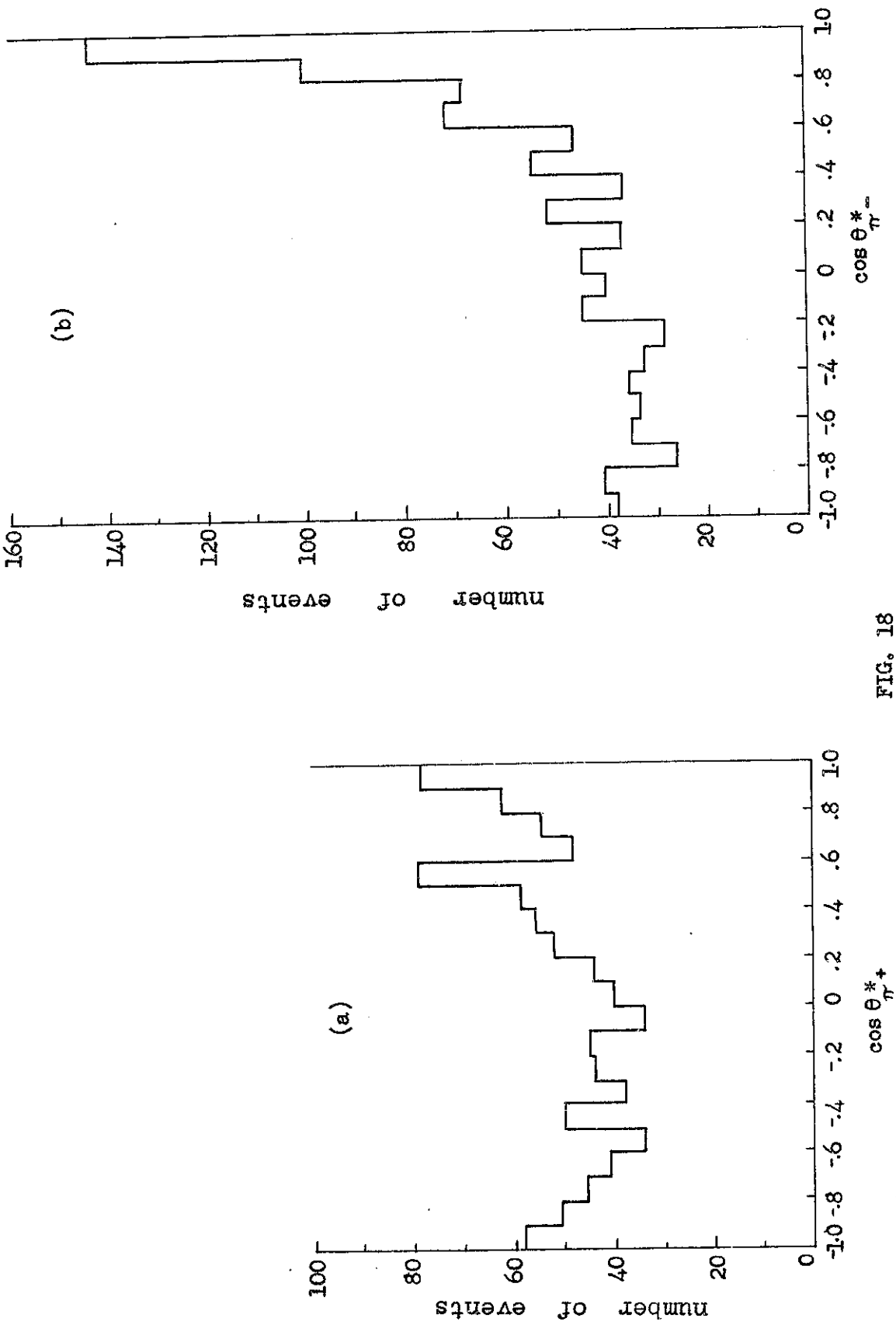
(a)
number of events
100
80
60
40
20
0
-1.0 -.8 -.6 -.4 -.2 0 .2 .4 .6 .8 1.0
cos θ*π+
(b)
number of events
160
140
120
100
80
60
40
20
0
-1.0 -.8 -.6 -.4 -.2 0 .2 .4 .6 .8 1.0
cos θ*π−

FIG. 18